LA-UR 91-1829

LA-UR--91-1829

DE91 013368

Los Alamos National Laboratory is operated by the University of California for the United States Department of Energy under contract W-7405-ENG-36

TITLE: Imaging of Reservoirs and Fracture Systems Using Microearthquakes Induced by Fluid Injections

AUTHOR(S): Michael Fehler, Leigh House, W. Scott Phillips, Lisa Block, and C.H. Cheng

SUBMITTED TO: Geothermal Resources Council

DISCLAIMER

Los Alamos Los Alamos National Laboratory
Los Alamos, New Mexico 87545

FORM NO. 836 R4
ST. NO. 2629 5/81

DISCLAIMER

IMAGING OF RESERVOIRS AND FRACTURE SYSTEMS USING MICROEARTHQUAKES INDUCED BY HYDRAULIC INJECTIONS

Michael Fehler [1] Leigh House[1] W. Scott Phillips[1] Lisa Block[2] C.H. Cheng[2]

(1) GeoEngineering Group, Los Alamos National Laboratory, Los Alamos, NM 87545
(2) Earth Resources Laboratory, Massachusetts Institute of Technology, Cambrigde, Ma.

ABSTRACT

Predicting the future performance of a geothermal reservoir and planning a strategy for increasing productivity from the reservoir require an intimate knowledge of the fracture system through which geothermal fluids permeate. Indirect methods, such as the use of tracers and modeling of thermal drawdown, can be used to infer bulk fracture system properties. These methods, however, provide no means for determining the locations of the fractures that comprise the system. Wellbore geophysical logs can be used to infer the locations of fractures intersecting the wellbores but provide no information about the fracture system away from the wellbore. Microearthquakes often accompany hydraulic fracturing as well as normal production activities in geothermal fields. The waveforms from these microearthquakes provide valuable information that can be used to infer the three-dimensional structure of the fracture system in the reservoir. The locations of the microearthquakes can be used to infer the presence of large fractures along which shear slip has occurred. Tomographic imaging using arrival times of the seismic waves, provides a three-dimensional image of the P and S wave velocity structure of the reservoir. These velocities yield information about the presence of microfractures in the rock. Waveform stacking methods can be used to both corroborate seismic velocities and image seismic scatterers in the reservoir. The most prominent seismic scatterers are likely to be fluid-filled fractures. Thus, seismic data provide information about a fractures over a large scale range which can be of use in reservoir engineering.

INTRODUCTION

Hydraulic fracturing is used extensively to increase the productivity of oil and gas wells, as well as in the development of geothermal resources. Subsequent to the hydraulic fracturing, if information about the fractured rock volume is needed, active seismic methods such as vertical seismic profiling (VSP) and crosswell tomography may be used along with single well logging. Imaging of the fractured region using active seismic methods is limited, however, by the narrow aperture (range of directions) of the source-receiver seismic ray paths, the small rock volumes sampled, and the limited energy of the artificial sources (particularly shear wave sources) used. Well logging can provide information about near-wellbore fractures, but offers no reliable information about the fracture system away from the wells. If, on the other hand, microearthquakes induced by hydraulic fracturing could be used as sources for probing the fractured rock volume, considerable improvement in source-receiver ray distribution, as well as substantially greater source excitation (particularly for shear waves) could be achieved. Because they are more strongly affected by the presence of fluids in rock, S (shear) waves are a more powerful diagnostic tool for studying hydraulically fractured rock than are P (compressional) waves.

Microearthquakes accompany many hydraulic injections [Albright and Pearson, 1982; Pine and Batchelor, 1984; Sarda, et al., 1988] as well as production from some gas fields [Pennington et al., 1986; Doser, et al., 1991] and geothermal fields [Zucca, et al., 1990; Block, 1991]. Arrival times of P and S waves from these induced microearthquakes have been used to locate the microearthquakes and to infer the orientation and dimensions of the fracture systems that were created by the hydraulic injections [Fehler, et al., 1987; House, 1987]. Although previous studies have mainly been concerned only with locating the induced microearthquakes, the arrival time data and the rest of the waveforms contain considerable information about the rock through which the seismic waves travel. Both the travel times of the direct P and S waves and the waveforms themselves contain information about the spatial heterogeneity of the rock. In addition, the portions of the waveforms after the first arrivals (termed coda) consist of conversions and reflections from fractures or other heterogeneities in and near the reservoir.

We are taking two approaches for inferring the properties of the fracture system in a hydraulically fractured reservoir from microearthquake data: tomography and waveform stacking. The tomographic method is being applied to the arrival times of P and S waves from the microearthquakes to simultaneously locate the microearthquakes and determine the P and S wave velocity structure of reservoirs in three dimensions. In addition, waveform stacking will be applied to determine the P and S wave velocities within selected regions of the hydraulically fractured rock. We will also apply waveform stacking to determine locations of inhomogeneities, such as fluid-filled fractures, that produce coherent large-amplitude signals in the coda. As a first step, we are testing these methods on data collected during a massive hydraulic fracturing experiment conducted as part of the Department of Energy Hot Dry Rock (HDR) Geothermal Energy Development Program. Our dataset consists of travel times and waveforms recorded from over 11,000 well located microearthquakes from that hydraulic fracturing operation.

The information that can be extracted by performing tomographic reconstruction of travel time data and stacking of the waveforms to image boundaries and interfaces will be extremely valuable to understanding the detailed properties of the geothermal reservoir involved. By analyzing data obtained during different time intervals, we can obtain information about

temporal changes in the structure of the reservoir, which can be used to better characterize the evolution of the reservoir and improve future production. Such information would be of major benefit to reservoir engineers in enhancing production from hydraulically fractured reservoirs as well as to the understanding of the hydraulic fracturing process itself.

SEISMICITY ACCOMPANYING HYDRAULIC FRACTURING

There have been numerous accounts of seismic events accompanying hydraulic fracturing since the first reports by Albright and Hanold [1976]. Observations on a small scale (less than 10 meter samples) have been made by Majer and Doe [1986] and Niitsuma, et al. [1987]. Observations in larger scale environments, up to 1 km, have been reported by Pine and Batchelor [1984], Sarda, et al. [1988], Talebi and Cornet [1987], and Kobayashi [1987]. Most of the observations have led to the conclusion that the seismic events are caused by shear slip along fault planes [House, et al., 1985, House and Jensen, 1987], although Fehler and Bame [1985] and Bame and Fehler [1986] reported observations of events that they interpreted to be due to the tensile opening of fractures. More recently, Ferrazzini, et al. [1990] have modeled these tensile events and estimated the dimensions of the open fractures through which fluid is in easy communication. The dimensions of the shear fractures have been reported by Pearson [1982] and Fehler and Phillips [1991].

Investigators working on the Department of Energy Hot Dry Rock Geothermal Energy Project have observed microearthquakes accompanying many of the hydraulic stimulations of the man-made geothermal reservoir [Albright and Pearson, 1983; Keppler, et al., 1983; Fehler, 1989]. Since these microearthquakes occur throughout the volume of the reservoir, they have the potential to provide information about the structure and thermal drawdown of the reservoir. Figure 1 shows the locations of a subset of the microseismic events determined by House [1987] to accompany a massive hydraulic fracturing operation conducted in the Fenton Hill Hot Dry Rock Reservoir. Locations of more than 11000 events that occurred during this massive hydraulic fracturing operation have been determined. Fehler [1989] has summarized the locations of microseismic events found to accompany other recent hydrofracturing operations in the Fenton Hill reservoir. He used the locations in a statistical scheme to determine planes along which the earthquakes cluster and interpreted these planes to be major flow paths in the reservoir.

TRAVEL TIME TOMOGRAPHY

Travel time tomography has been used extensively to infer the spatial variations of seismic velocities in the earth. The major effort in the oil and gas industry has been in transmission tomography using the crosswell geometry. Numerous methods have been proposed to reduce the adverse relationship between noise in the data and the high frequency noise in the images [for a discussion, see Phillips and Fehler, 1991]. The problem arises because of the limited resolution of the data and the resulting nonuniqueness of the final model. In the crosswell geometry, the nonuniqueness arises because rays that travel at angles subparallel to the boreholes cannot be sampled.

Data from induced microearthquakes contain additional rays that, in principle, allow much better resolution of the rock structure by travel time tomography than is possible using VSP or crosswell techniques. Since the microearthquakes are located throughout the volume of rock to be imaged, rays pass through the reservoir in a larger range of angles and sample a larger rock volume than is possible using artificial sources. Use of microearthquake data allows a fully three-dimensional image of the reservoir to be obtained. Additionally, since the microearthquakes excite strong S waves, both the P and S wave velocity structure of the reservoir can be determined. Knowledge of both velocities can be used to more reliably determine the locations of anomalous regions, such as those containing liquids or gas, and/or newly created fractures in the reservoir.

Our approach is to simultaneously determine the locations of the microearthquakes and find the three-dimensional P and S wave velocity structures. In realistic field operations, the number of observation wells will necessarily be limited. This limitation will reduce the resolution of the velocity structure and produce trade-offs between microearthquake locations and the velocity structure. We have thus resorted to including as much *a priori* information in the inversion scheme as possible to reduce the trade-offs and improve the resolution obtained [Block, et al., 1990]. Constraint on velocity smoothness using a second difference scheme and penalties for velocities increasing above the known velocity outside the stimulated region and for low Vp/Vs ratios have been implemented. Tests to investigate the relative importance of constraints and penalties have been made.

We found a spatial resolution in velocity of approximately 100-200 m from the data used. We also found clear evidence for a zone of low S-wave velocity in the region surrounding the injection zone. Locations of the microearthquakes deep in the reservoir moved systematically towards a more vertical and north-south alignment compared to the original locations obtained using a homogeneous velocity model. Locations of the deeper events moved more than those of the shallow events because ray paths from the deeper events to the seismic stations passed through a more heterogeneous velocity structure than did those from the shallower events. A horizontal slice through the S-wave velocity structure at a depth near the fluid injection zone is shown in Figure 2. Epicenter views of event locations occurring within 50 m depth of the slice determined using a homogeneous velocity structure and the locations determined by the joint epicenter-tomographic inversion are also shown.

EXPLOITING THE WAVEFORMS: STACKING METHODS

The waveforms of the induced microearthquakes can be analyzed to yield detailed information about the internal structure of the fractured volume. Our goals are first, to obtain independently from the travel time tomography, seismic velocities in selected sub-volumes within the fractured volume, and second, to identify and locate some of the more prominent fluid-filled fractures. Seismic velocities within the sub-volumes will be uniquely determined from stacking waveforms of the induced microearthquakes and can then be used as additional *a priori* information to minimize the nonuniqueness in the travel time tomography. Individual prominent fractures or joints will be identified and located from their signatures as notable distinct arrivals in the P and S wave codas. Knowledge of the locations of these features will help to improve models of the fractured volume as well as understanding of the fluid paths.

Results of both the velocity and scattering analyses can be severely degraded by uncertainties in the locations of the microearthquakes that are used and by variations in the seismic radiation patterns among the events. Therefore, microearthquake locations have been screened for reliability by a simple relocation process. Results of the stacking can also be degraded by variations in the focal mechanisms of the events used in the analysis. Similarity of focal mechanisms has been qualitatively judged from plots of the entire microearthquake seismograms.

Stacking for velocities

Because of the need to help constrain the nonuniqueness of the velocity tomography, a simple scheme has been devised to determine the seismic velocities within selected sub-volumes of the fractured rock [Phillips and House, 1990]. This scheme exploits the concept of seismic reciprocity to allow a conceptual interchange of sources (normally the induced microearthquakes) with receivers (normally the recording instruments) [Spudich and Bostwick, 1987] as shown in Figure 3. Thus, instead of having many sources and only a few receivers (which was the experimental situation), we can consider that we have many receivers and only a few sources (the reciprocal situation). After the conceptual interchange, we can stack the waveforms of the microearthquakes to obtain the direction of approach of the (reciprocal) waves travelling from the recording instrument to the microearthquakes, as well as their apparent velocities. Stacking is done for each of a range of P and S velocities, and for all possible wavefront directions. Taking the velocities that produced the maximum stack amplitudes (individually for P and S), the earthquakes are relocated, and the stacking is repeated. The stack, relocate, stack process is continued until a maximum amplitude is obtained for the resulting stack.

In our first test, we used waveforms from a cluster of 52 microearthquakes to investigate seismic velocities in a cube about 80 m on a side. Meeting the stack-relocate termination criteria described above took four iterations. We obtained a P wave velocity of 5.2 km/s, and an S wave velocity of 3.2 km/s in the cube. Plots of example seismograms and the stacked traces obtained are shown in Figure 4. The velocities obtained from the cube compare to intact rock velocities of 5.92 and 3.5 km/s, respectively. While the lower S wave velocity in the cube was expected to result from the injected volume of water, the lowered P wave velocity is surprising, and suggests the presence of partially saturated joints or fractures.

Stacking for Coda Arrivals

The water injected during a hydraulic fracturing operation is not accommodated uniformly throughout the rock, but rather opens some joints or fractures in response to the fluid pressure. The apertures of even the largest joints or fractures may be only a few mm, and thus difficult to identify with conventional methods. Nevertheless, these joints or fractures may be effective at reflecting or scattering seismic waves, particularly S waves [e.g. Aki, et al., 1982], and these reflected or scattered waves may be seen in the P and S wave codas.

By use of another stacking scheme, we can selectively enhance the arrivals that result from scattering. Development and application of the method was motivated by the presence of prominent arrivals in the early coda of some seismograms (see Figure 4A).

The method consists of two steps. First is a reconnaissance step, in which a 3-D grid of possible scattering locations is chosen, in a manner similar to the 2-D procedure used by Lynnes and Lay [1989] to look for near surface scatterers at the Nevada Test Site. To minimize the influence of small errors in velocities and event locations, envelopes of the seismograms may be used, rather than the seismograms themselves. Next, for each point in the 3-D grid, each microearthquake seismogram is moved out by an amount corresponding to the arrival time of the corresponding scattered wave. The envelope value at the moved-out time is added to the cumulative stack value for the grid point. The result of this procedure is a 3-D grid of envelope stack values.

Likely scattering surfaces will be identified from the results of the 3-D grid reconnaissance. The locations and orientations of these surfaces will be refined by a second pass, this one using scattering surfaces rather than individual grid points.

The most prominent scattering surfaces identified in this second stacking presumably will correspond to prominent fluid paths. The correspondence can be tested by comparison to other available data, for example the three point planes identified from the microearthquake location dataset [Fehler, et al., 1987]. Further interpretation of the scattering results can take advantage of the theoretical work of Fehler [1982], Coutant [1989], and Pyrak-Nolte, et al., [1990] to infer the properties of the joints or fractures identified. These properties can then be compared to fluid-flow models of the fractured volume.

ACKNOWLEDGMENTS

This work was funded by the U.S. Department of Energy, Office of Basic Energy Sciences, which is headed by Bill Luth. This work was carried out under the auspices of the U.S. Department of Energy under contract W-7405-ENG-36.

REFERENCES

Aki, K., M. Fehler, R.L. Aamodt, J.N. Albright, R.M. Potter, C.F. Pearson, and J.W. Tester, 1982. Interpretation of seismic data from hydraulic fracturing experiments at the Fenton Hill, New Mexico, Hot Dry Rock geothermal site, *J. Geophys. Res.*, *87*, 936-944.

Albright, J., and R. Hanold, 1976. Seismic mapping of hydraulic fractures in basement rocks, *Proc. 2nd ERDA Enhanced Oil and Gas Recovery Symposium.*

Albright, J.N., and C.F. Pearson, 1982. Acoustic emissions as a tool for hydraulic fracture location: experience at the Fenton Hill hot dry rock site, *Soc. Petr. Eng. J.*, *22*, 523-530.

Bame, D. and M. Fehler, 1986. Observations of long period earthquakes accompanying hydraulic fracturing, *Geophys. Res. Letters*, 13, 149-152.

Block, L., 1991. Joint hypocenter-velocity inversion of local earthquake arrival time data in two geothermal regions, PhD Thesis, Massachusetts Institute of Technology.

Block, L., C.H. Cheng, M. Fehler, and W.S. Phillips, 1990. Inversion of microearthquake arrival time data at the Los Alamos Hot Dry Rock Reservoir, Society of Exploration Geophysicists, Expanded Abstracts of the 1990 Technical Program, 1226-1229.

Coutant, O., 1989. Numerical study of the diffraction of elastic waves by fluid-filled cracks, *J. Geophys. Res.*, *94*, 17805-17818.

Doser, D., M. Baker, and D. Mason, 1991. Seismicity in the War-Wink gas field, Delaware basin, west Texas, and its relationship to petroleum production, preprint.

Fehler, M., 1982. Interaction of seismic waves with a viscous liquid layer, *Bull. Seismol. Soc. Am.*, *72*, 55-72.

Fehler, M., 1989. Stress control of seismicity patterns observed during hydraulic fracturing experiments at the Fenton Hill Hot Dry Rock geothermal energy site, New Mexico, *Int. J. Rock Mech. Mining Sciences and Geomech Abstr.*, 26, 211-219.

Fehler, M. and D. Bame, 1985. Characteristics of Microearthquakes accompanying hydraulic fracturing as determined from studies of Spectra of Seismic Waveforms, *Trans. Geotherm. Res. Council*, 9, part II, 11-16.

Fehler, M., L. House, and H. Kaieda, 1987. Determining planes along which earthquakes occur: Method and application to earthquakes accompanying hydraulic fracturing, *J. Geophys. Res.*, *92*, 9407-9414.

Fehler, M. and W. S. Phillips, 1991. Simultaneous inversion for Q and source parameters of microearthquakes accompanying hydraulic fracturing in granitic rock, *Bull. Seism. Soc. Am.*, 81, 553-575.

Ferrazzini, V., B. Chouet, M. Fehler, and K. Aki, 1990. Quantitative analysis of long-period events recorded during hydraulic fracturing experiments at Fenton Hill, New Mexico, *J. Geophys. Res.* 95, 21871-21884.

House, L., H. Keppler, and H. Kaieda, 1985. Seismic studies of a massive hydraulic fracturing experiment, *Trans. Geotherm. Res. Counc.*, 9 (part II), 105-110.

House, L., 1987. Locating microearthquakes induced by hydraulic fracturing in crystalline rock, *Geophys. Res. Lett.*, *14*, 919-921.

House, L., and B. Jensen, 1987. Focal mechanisms of microearthquakes induced by hydraulic injection in crystalline rock (abstract) *EOS, Trans. Am. Geophys. Un.*, 68, 1346.

Keppler, H., C. Pearson, R. Potter, and J. Albright, 1983. Microearthquakes induced during hydraulic fracturing at the Fenton Hill HDR site: the 1982 experiments, *Trans. Geotherm. Res. Counc.*, 7, 429-433.

Kobayashi, H., 1987. Hydraulic fracturing tests to make geothermal reservoir for hot dry rock development at Hijiori, Japan, *Trans. Geotherm. Res. Counc.*, 11.

Lynnes, C.S., and T. Lay, 1989. Inversion of P coda for isotropic scatterers at the Yucca Flat test site, *Bull. Seismol. Soc. Am.*, *79*, 790-804.

Majer, E., and T. Doe, 1986. Studying hydraulic fractures by high frequency seismic monitoring, *Int. J. Rock Mech. Min Sci. and Geomech Abstr.*, 23, 185-199.

Niitsuma, H., N. Chubachi, and M. Takanohashi, 1987. Acoustic emission analysis of a geothermal reservoir and its application to reservoir control, *Geothermics*, 16, 47-60.

Pearson, C., 1982, Source parameters and a magnitude-moment relationship from small local earthquakes observed during hydraulic fracturing in crystalline rock, *Geophys. Res. Letters*, 9, 404-407.

Pennington, W., S. Davis, S. Carlson, J. DuPree, and T. Ewing, 1986. The evolution of seismic barriers and asperities by the depressuring of fault planes in oil and gas fields of south Texas, *Bull. Seismol. Soc. Am.*, *76*, 939-948.

Phillips, W.S., and M. Fehler, 1991. Traveltime tomography: a comparison of popular methods, in press, *Geophysics*.

Phillips, W.S., and L. House, 1990. An array method to estimate seismic velocities in a cluster of microearthquakes, *EOS, (Trans. Am. Geophys. Union), 43*, 1446-1447.

Pine, R.J., and A.S. Batchelor, 1984. Downward migration of shearing in jointed rock during hydraulic injections, *Int. J. Rock Mech. Min. Sci. & Geomech. Abstr.*, *21*, 249-263.

Pyrak-Nolte, L., L. Myer, and N. Cook, 1990. Transmission of seismic waves across single natural fractures, *J. Geophys. Res.*, 95, 8617-8638.

Sarda, J.-P., P.J. Perreau, and J.-P. Deflandre, 1988. Acoustic emission interpretation for estimating hydraulic fracture extent, SPE paper 17723, presented at SPE Gas Technology Symposium, Dallas, TX, June 13-15.

Spudich, P., and T. Bostwick, 1987. Studies of the seismic coda using an earthquake cluster as a deeply buried seismograph array, *J. Geophys. Res.*, *92*, 10526-10546.

Talebi, S., and F. Cornet, 1987. Analysis of microseismicity induced by a fluid injection in a granitic rock mass, *Geophys. Res. Letters*, 14, 227-230.

Zucca, J, L. Hutchings, and M. Start, 1990. P-wave velocity and attenuation tomography at the Geysers geothermal field and its relation to the steam reservoir (abstract), *EOS, (Trans. Am. Geophys. Union), 43*, 1467.

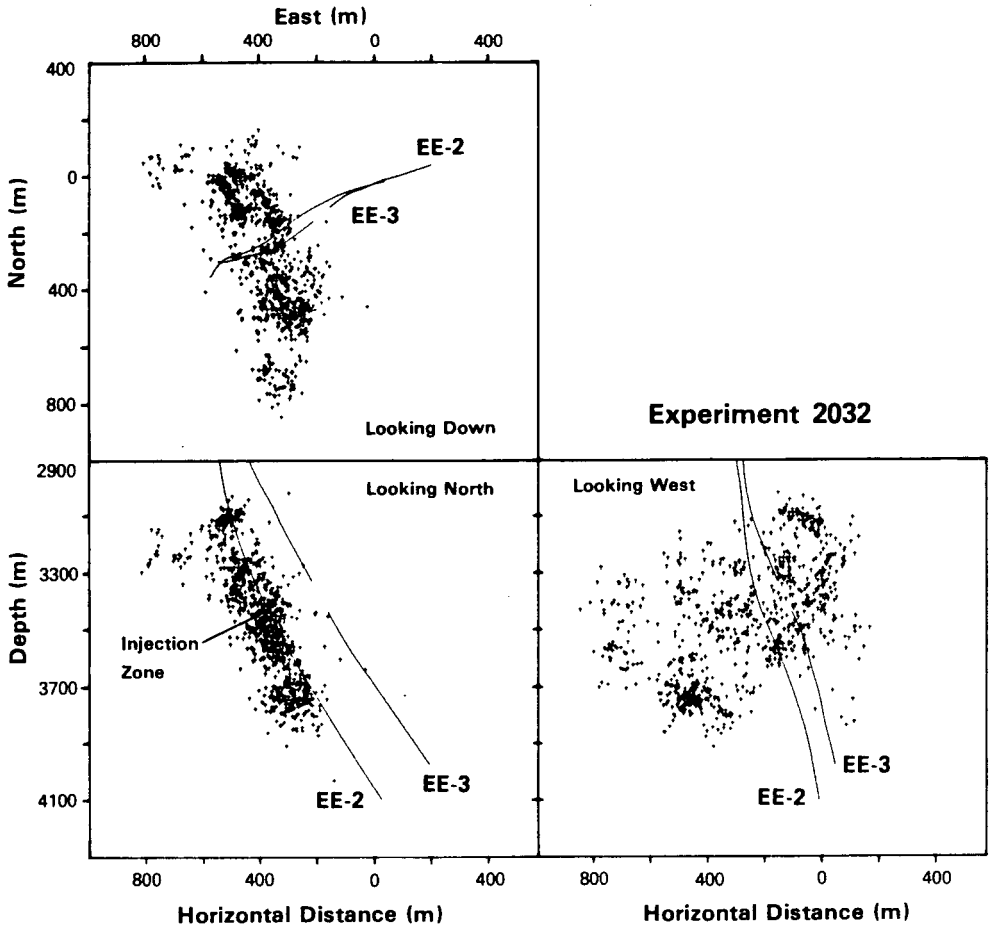

Figure 1. Three orthogonal views showing locations of events accompanying the massive hydraulic fracturing experiment as found by House [1987]. Upper left: plan view. Lower left: vertical cross section projected onto an east-west plane. Lower right: vertical cross section projected onto a north-south plane. There is no vertical exaggeration in the figures. The trajectory of the injection wellbore, EE-2, and a second nearby wellbore, at the time of the hydraulic fracturing operation are shown. The open hole injection zone in EE-2 is labeled.

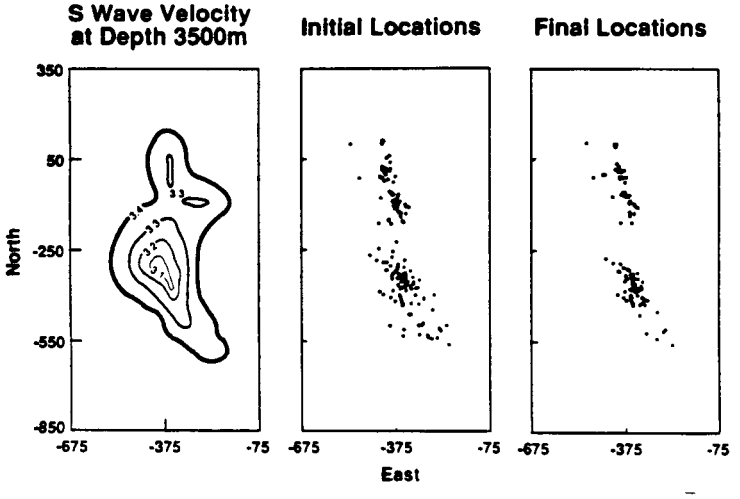

Figure 2. Results of simultaneous determination of microearthquake locations and velocity structure. Left hand box shows S wave velocity at a depth of 3500 m below the surface, at the depth where the fluid was injected into the reservoir. Middle box shows locations of microearthquakes determined with a homogeneous velocity structure (Vp of 5.92 km/s, Vs of 3.50 km/s) and whose depths are within 50 m of the 3500 m depth. Right hand box shows locations in same depth interval determined by the simultaneous inversion. Note that the final locations form a tighter cluster than do the initial locations.

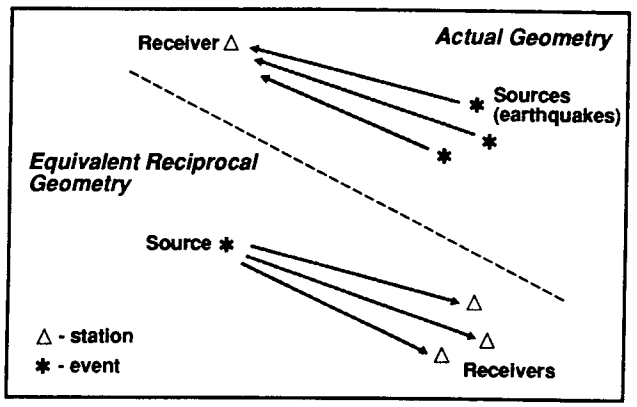

Figure 3. Conceptual view of seismic reciprocity. The upper portion of the figure shows the actual geometry in which data are collected. There are many sources and a single receiver. In the lower portion of the figure, we have conceptually exchanged the sources and receivers so that we can consider that we have many receivers monitoring a single source.

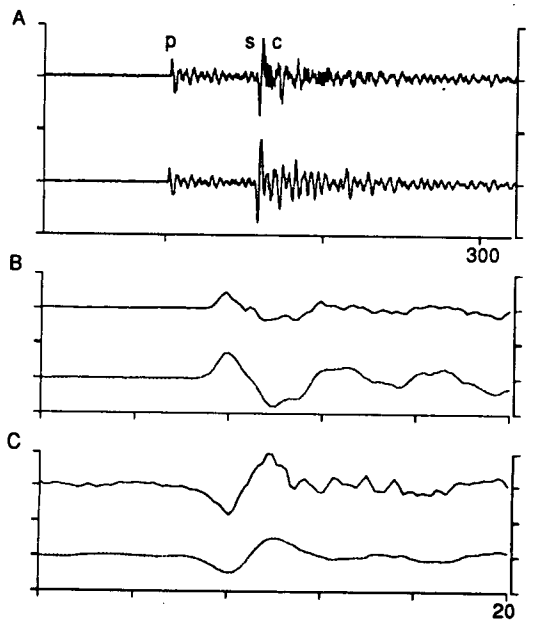

Figure 4. (A) Examples of raw (unstacked) traces from two microearthquakes. Note similarity of the seismograms, despite an approximate factor of 2 difference in sizes of the microearthquakes. P and S arrivals are identified (labelled 'p' and 's'), as are some prominent arrivals in the early S coda (labelled 'c'). Tick marks on time axis are 100 ms apart.
(B) P wave data: top is single trace, bottom is stack of traces from 52 microearthquakes at Vp of 5.2 km/sec. Tick marks on time axis are 4 ms (20 samples) apart.
(C) S wave data: as (B). Stack is for Vs of 3.2 km/sec.